BILINGUAL PUBLISHING GROUP

Artificial Intelligence Advances

https://journals.bilpubgroup.com/index.php/aia

ARTICLE

Research on Fault Diagnosis of Motor Rolling Bearing Based on Improved Multi-Kernel Extreme Learning Machine Model

***Guojun Zhang*[1], *Tong Zhou*[2,*], *Weidong Huang*[3,4]**

[1]*Quadrant international Inc., San Diego, CA 92121, USA*

[2]*Air China Cargo Co., Ltd., Beijing 101318, China*

[3]*GAC FIAT CHRYSLER Automobiles Co., Ltd., Changsha 410100, China*

[4]*HYCAN Automobile Technology Co., Ltd., Guangzhou 510000, China*

ABSTRACT

Motors play a crucial role in energy conversion and are essential components of mechatronic systems. However, diagnosing faults in rolling bearings during motor operation presents significant challenges, making it difficult to achieve high accuracy in fault identification. To address these challenges, this paper introduces a novel intelligent diagnostic method based on an enhanced multi-kernel extreme learning machine (ELM) model. While the ELM model is widely used for diagnosing motor rolling bearing faults, it often struggles to classify complex vibration data. To improve its performance, this study proposes a multi-kernel ELM (MKELM) model that integrates three traditional kernel functions: Gaussian, polynomial, and perceptron kernels. Additionally, to overcome the challenges posed by the numerous parameters and the risk of local optima in the MKELM model, the kernel parameters were optimized using the Grey Wolf Optimization (GWO) algorithm, resulting in the GWO-MKELM algorithm. Finally, the GWO-MKELM algorithm was applied to diagnose motor rolling bearing faults. Experimental results show that this method achieves a 99.6% accuracy rate and effectively identifies various types of bearing faults.

Keywords: Mechatronics; Motor structure; Rolling bearings; Intelligent optimization algorithm; Fault diagnosis

*CORRESPONDING AUTHOR:

Tong Zhou, Air China Cargo Co., Ltd., Beijing 101318, China; Email: zhoutong@airchinacargo.com

ARTICLE INFO

Received: 12 June 2023 | Revised: 10 July 2023 | Accepted: 15 July 2023 | Published Online: 14 August 2023

DOI: https://doi.org/10.30564/aia.v5i1.7489

CITATION

Zhang, G., Zhou, T., Huang, W., 2023. Research on Fault Diagnosis of Motor Rolling Bearing Based on Improved Multi-Kernel Extreme Learning Machine Model. Artificial Intelligence Advances. 5(1): 41–48. DOI: https://doi.org/10.30564/aia.v5i1.7489

1. Introduction

Motors are critical components in mechatronic systems, playing a key role in energy conversion. Rolling bearings, as essential parts of motor structures, directly influence overall motor performance and lifespan[1, 2]. Therefore, timely and accurate fault diagnosis of rolling bearings during operation is vital. Common faults in motor rolling bearings include failures in the outer ring, inner ring, rolling elements, and cage. Numerous studies have been conducted to identify these faults, among them, many diagnostic methods rely on time-frequency signal analysis, which extract characteristic features from vibration signals. Unfortunately, these methods often encounter challenges in feature extraction and frequently suffer from low accuracy. Thus, developing an efficient fault diagnosis method for motor rolling bearings is crucial for maintaining motor integrity[3, 4]. Leveraging distributed data parallelism in GANs can enhance fault diagnosis efficiency in large-scale data processing, advancing the field[5, 6].

With the continuous advancement of AI algorithms, methods such as Support Vector Machines (SVM), Kernel Extreme Learning Machines (KELM), and Neural Networks have been proposed and successfully applied in motor rolling bearing fault diagnosis. Data-driven intelligent algorithms have proven effective in optimizing supply chain management and industrial clusters, offering potential improvements for fault diagnosis[7–9]. Among them, KELM is particularly favored for its high computational efficiency, fast learning speed, and resistance to local optima, making it widely used in various motor bearing fault diagnostics[10–12]. However, the KELM model often relies on a single kernel function, limiting its performance in classifying complex motor bearing vibration data and negatively impacting diagnostic accuracy. To overcome these limitations, researchers have made several improvements to the KELM model. For example, Chen Chi et al.[13] established a hybrid KELM model by combining Gaussian radial basis and polynomial kernel functions for transformer fault diagnosis. Experimental results showed that the hybrid model significantly improved classification accuracy, but it struggled with low computational efficiency. Huang Guangbin et al. advanced the KELM by integrating polynomial and radial basis functions, establishing a Multi-Kernel Extreme Learning Machine (MKELM) model. They optimized the model's parameters using the Particle Swarm Optimization (PSO) algorithm, which enhanced the MKELM model's recognition accuracy[14, 15]. Meanwhile, the MKELM model still faces challenges in selecting optimal kernel parameters, leading to lower recognition accuracy. To address this issue, Wang Jing et al.[16] proposed a method to optimize the kernel parameters of the MKELM model using the Cuckoo Search algorithm, aiming to enhance classification accuracy. Meanwhile, green technology innovations are increasingly impacting China's chemical industry, driving further advancements in motor fault diagnosis technology[17, 18]. However, this optimization algorithm still suffers from low computational efficiency and has a tendency to get trapped in local optima.

The studies above demonstrate that developing an MKELM model is effective, and optimizing its kernel parameters using intelligent algorithms can further improves the fault diagnosis accuracy. Thus, this study is conducted to establish a more efficient ELM for bearing fault diagnosis.

2. Motor structure design and bearing fault diagnosis methods

2.1 Motor structure design

Motors are vital components in industrial automation, and their rational design along with timely fault diagnosis is essential for ensuring production safety and enhancing equipment efficiency. At the same time, material innovations have provided valuable insights for motor structure design, particularly in enhancing durability and heat dissipation[19–21]. This study focuses on a wound-rotor induction motor, and its structural components illustrated in **Figure 1**[22].

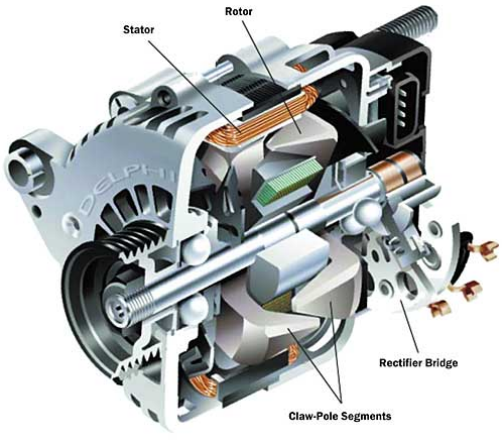

Figure 1. Structure of the wound-rotor asynchronous motor.

2.2 Bearing fault diagnosis methods

Rolling bearings are critical components of a motor's transmission system, and their operating condition directly affects the overall performance and lifespan of the motor. To prevent motor failures and ensure smooth production, diagnosing faults in rolling bearings is essential. Common diagnostic methods include vibration signal analysis, sound monitoring diagnosis, lubrication condition inspection, and temperature and wear monitoring. The following sections describe the above diagnostic methods for motor rolling bearings fault diagnosis[23–25].

(1) Vibration Signal Analysis

Vibration signal analysis is a widely used and effective method for diagnosing faults in rolling bearings. In recent years, deep learning has achieved significant success in image recognition, and its application in complex signal processing offers new directions for bearing vibration analysis[26]. By installing vibration sensors, real-time data from the bearing's operation can be collected and analyzed. Common vibrational-based analysis methods include time analysis, frequency analysis, and time-frequency analysis.

(2) Sound monitoring diagnosis

Sound monitoring is a straightforward and easy-to-implement method for fault diagnosis. Acoustic sensors, such as microphones, capture the sound signals generated by the bearing during operation. The frequency, tone, and volume of these signals are captured and analyzed to assess the bearing's condition. For example, abnormal noises caused by bearing wear, poor lubrication, or foreign objects can indicate faults.

(3) Lubrication condition inspection

The lubrication condition is a key factor affecting the operational quality of rolling bearings, making regular lubrication checks essential. These checks involve assessing the quantity, quality, and formation of the oil film. One approach is to examine the lubricant's color and clarity, while testing its viscosity and acidity offers further insights. Lubrication oil analysis can also detect metal wear particles and contaminants. These measures are vital for early detection of potential issues arising from insufficient lubrication.

(4) Temperature and wear monitoring

Temperature and wear are two critical parameters that indicate the operational state of bearings. By installing temperature sensors, the temperature variations of the bearings can be monitored in real time, allowing for the timely detection and prevention of heat-induced damage. Additionally, regular inspections of bearing wear are essential, including measuring clearance and checking for wear marks on rolling elements and raceways. These inspections help assess the remaining life of the bearings and determine whether replacement is necessary.

3. GWO-MKELM intelligent pattern recognition algorithm

3.1 Grey Wolf Optimizer (GWO)

In 2014, the renowned scholar Mirjalili et al.[27] proposed an intelligent optimization algorithm called the Grey Wolf Optimizer (GWO), which simulates the hunting behavior of wolf packs. This algorithm has several advantages compared with its peers, including a small number of initial parameters, high computational efficiency, and strong optimization performance.

In the GWO, wolves are categorized into four different groups: Wolves α, responsible for making decisions during the hunting. The rest groups are classified as beta (β) and delta (δ).

The computational steps of the Grey Wolf Optimization algorithm primarily consist of two phases: encircling and hunting.

(1) Encircling

During the hunt, grey wolves first encircle their target prey, confining it within the pack's range. The distance between the prey and the grey wolves is expressed by Equation (1), while the position of the wolf pack at the t-th iteration can be represented by Equation (2):

$$D = |C \cdot X_p(t) - X(t)| \tag{1}$$

$$X(t+1) = X_p(t) - A \cdot D \tag{2}$$

where t represents the number of iterations, $X_p(t)$ is the position of the optimal solution, D is the distance between the wolf pack and the target prey, and $X(t+1)$ denotes the position of the wolf pack during the t-th iteration. A and C are corresponding coefficients, as shown in Equations (3) and (4).

$$A = 2a \cdot r_1 - a \tag{3}$$

$$C = 2 \cdot r_2 \tag{4}$$

where a is convergence factor, r_1 and r_2 represent random numbers in range [0, 1].

(2) Hunting

After encircling the prey, wolves β and δ, under the leadership of the wolves α, proceed to capture the target. In this process, the positions of all wolves change randomly, and the prey's position is updated based on the location of each wolf. The specific steps for updating the positions are shown in Equations (5) and (6).

$$\begin{cases} D_\alpha = |C_1 X_\alpha(t) - X(t)| \\ D_\beta = |C_2 X_\beta(t) - X(t)| \\ D_\delta = |C_3 X_\delta(t) - X(t)| \end{cases} \tag{5}$$

$$\begin{cases} X_1 = X_\alpha(t) - A_1 D_\alpha \\ X_2 = X_\beta(t) - A_2 D_\beta \\ X_3 = X_\delta(t) - A_3 D_\delta \end{cases} \tag{6}$$

$$X_p(t+1) = \frac{X_1 + X_2 + X_3}{3} \tag{7}$$

where D_α, D_β, D_δ is the step lengths of the current wolves α, β, and δ during the hunting.

Specifically, when $A \geq 1$, the wolf pack conducts a range search to enlarge the hunting area, which is called global search. When $A < 1$, the wolf pack narrows the encircling area and focuses on attacking, corresponding to local search. The coefficient vector C, which takes values in the range [0, 2], assigns random weights that enhance the algorithm's random search capabilities, helping it avoid local optima.

3.2 Multi-Kernel Extreme Learning Machine model (MEKLM)

The MKELM model introduced in this paper composes of two steps: First, it linearly combines three traditional kernel functions, i.e., the Gaussian kernel, polynomial kernel, and perceptron kernel, to create a multi-kernel function. Next, this multi-kernel function is employed to classify the sample data using the spatial mapping method (illustrated in **Figure 2**), enabling efficient classification and recognition.

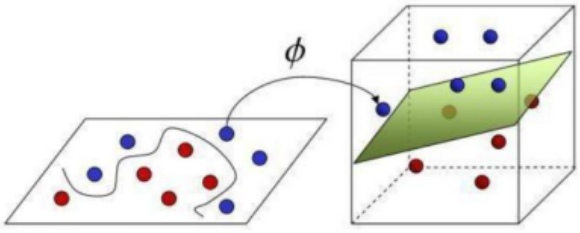

Figure 2. Spatial mapping transformation method of the kernel function.

(1) Polynomial kernel function

The polynomial kernel function is a classic global kernel in the MKELM model, recognized for its strong ability to handle complex data samples while requiring fewer initial parameters compared with other kernels. This kernel function is displayed in Equation (8).

$$K_1(x_i \cdot x_j) = [\alpha(x_i \cdot x_j) + \beta]^n \tag{8}$$

where $K_1(x_i \cdot x_j)$ represents the kernel function, x_i is the coordinates of the i-th point, x_j is the coordinates of the j-th point, α and β are the kernel parameters.

(2) Perceptron kernel function

The perceptron kernel function is a novel mapping kernel. It effectively handles nonlinear data and compresses the data while preserving its amplitude. The kernel function is shown in Equation (9).

$$K_2(x_i \cdot x_j) = tan[v(x_i \cdot x_j) + c] \tag{9}$$

where $K_2(x_i \cdot x_j)$ is the kernel function, x_i and x_j represents the coordinates of the i-th and j-th point, respectively.

Gaussian kernel function

The Gaussian kernel has several advantages, including a wide mapping space, a small number of initial kernel parameters, and high computational efficiency. This kernel function is shown below.

$$K_3(x_i \cdot x_j) = exp(-\gamma\delta(x_i \cdot x_j)) \tag{10}$$

$$\delta(x, y) = \sqrt{\sum_{i=1}^{n} (x_i - y_i)^2} \tag{11}$$

where $K_3(x_i \cdot x_j)$ is the kernel function, $\delta(x, y)$ is the Euclidean distance, γ is the kernel parameter.

This study utilizes a hybrid kernel function obtained by linearly combining the polynomial, perceptron, and Gaussian kernel functions. This approach not only enhances optimization performance but also ensures the algorithm's generalization capability. Consequently, the MKELM model demonstrates improved stability and accuracy in managing multi-class sample data. The expression for the MKELM algorithm is presented in Equation (12).

$$K = \frac{\sum_{i=1}^{3} q_i K_i}{\sum_{i=1}^{3} q_i} \tag{12}$$

where q_i is the product coefficient corresponding to the i-th kernel function, K_1 is the polynomial kernel function in Equation (8), K_2 is the perceptron kernel function in Equation (9), K_3 is the the Gaussian kernel function in Equation (10).

3.3 Algorithmic process of the GWO-MKELM intelligent pattern recognition method

The computational steps of the GWO-MKELM are as follows:

Step 1: Select the training sample.

Step 2: Classify the original training sample set using the MKELM model, generating a new sample set that includes the kernel function parameters of the MKELM model.

Step 3: Apply the GWO to the kernel parameters of the MKELM model.

Step 4: Input the optimized kernel function parameters (obtained from the optimization) into the MKELM model for retraining, resulting in optimal pattern recognition.

4. Steps for fault diagnosis of vibration signals in motor rolling bearings

Given the nonlinear characteristics and feature coupling of vibration signals in motor rolling bearings, this paper establishes a fault feature extraction and diagnosis method based on an improved MKELM model. The specific procedures for this fault diagnosis method are outlined below:

Step 1: Vibration signals are collected using an accelerometer placed on the motor.

Step 2: The original vibration signals of the motor rolling bearings are adaptively decomposed using the Empirical Mode Decomposition (EMD) method, resulting in a series of Intrinsic Mode Function (IMF) components.

Step 3: The correlation coefficients between each IMF component and the original vibration signal are calculated. According to statistic, higher correlation coefficient indicates greater fault-related information and contains less noise in corresponding IMF components. Therefore, the IMF components with higher correlation coefficients are selected for summation and reconstruction, ultimately yielding a refined rolling bearing vibrational signal.

Step 4: The Multiscale Fuzzy Entropy (MFE) algorithm is applied to the reconstructed vibration signal for fault feature extraction. This step identifies key fault information from the vibration signal and constructs the fault feature vectors used in the pattern recognition method.

Step 5: Finally, the GWO-MKELM is used for motor rolling bearing fault diagnosis.

5. Experimental verification of the proposed method

5.1 Data sources

Data from a motor bearing vibration simulation platform were utilized to evaluate the effectiveness of the proposed method[28]. The rolling bearing was operated under a load of 0 Hp, at a speed of 1750 r/min, and with a sampling frequency of 12 kHz. Spark erosion technology was employed to induce faults in the outer race, inner race, and rolling elements of the normal bearing, resulting in a damage diameter of 0.5336 mm. The test created three fault states for the motor rolling bearing[29], in addition to the normal state, yielding a total of four distinct states. **Figure 3** displays the examples of the vibration signals under different states.

5.2 Fault feature extraction based on EMD and MFE

First, the EMD decomposition was employed to the vibration signals. Specifically, the vibration signal of each state was divided into multiple IMF components. **Figures 4** and **5** display an example using the EMD decomposition for normal signal and inner ring fault signal, respectively.

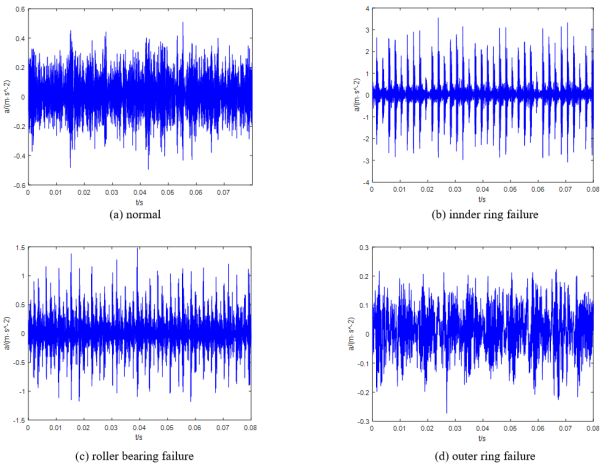

Figure 3. Time domain signals of motor rolling bearing under different states.

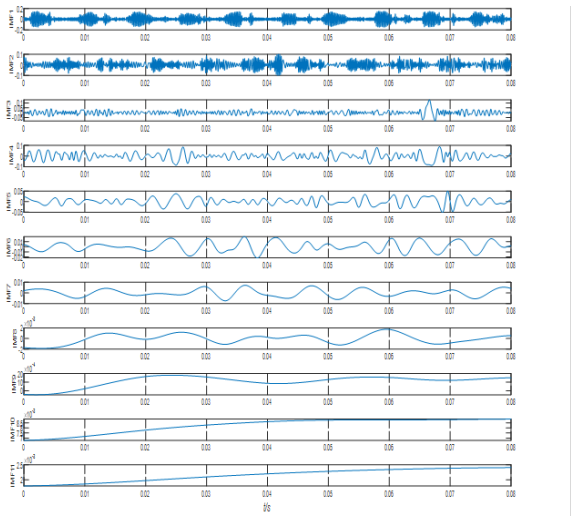

Figure 4. EMD decomposition of vibration signals under normal conditions.

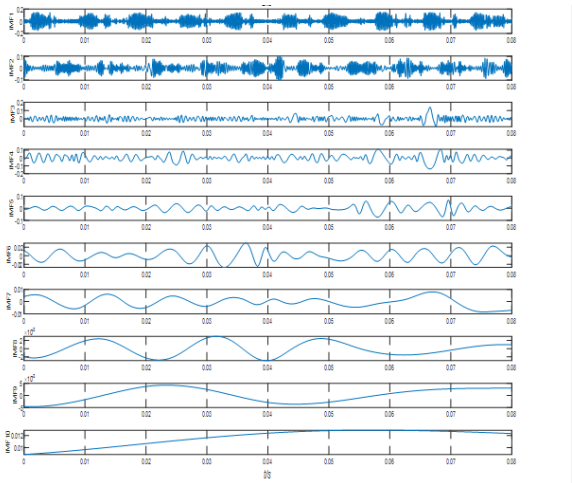

Figure 5. EMD decomposition of vibration signals under inner ring fault conditions.

Then, the correlation coefficients between each IMF component and the original signal were calculated. According to statistic, a higher coefficient indicates that the IMF signal contains more fault characteristic information and less noise. Thus, the first six IMF components were selected for further study due to their relatively high coefficients, as displayed in **Table 1**[30]. These IMF components were then summed and reconstructed to yield the refined vibration signal.

Table 1. Correlations of the first six IMF components with the original signal.

Fault type	The correlation coefficients between each IMF component and the original signal					
	IMF1	IMF2	IMF3	IMF4	IMF5	IMF6
Normal condition	0.4145	0.9312	0.7165	0.2310	0.4755	0.2265
Inner ring fault	0.3658	0.9468	0.7132	0.1245	0.3989	0.1745
Rolling element fault	0.4591	0.6548	0.8465	0.4726	0.4419	0.0895
Outer ring fault	0.3512	0.8825	0.8965	0.0961	0.4528	0.3796

Subsequently, the refined vibration signals were analyzed using the MFE method by entropy-based feature extraction[31], resulting in 20 fault characteristics from each sample data, as shown in **Table 2**. These values formed the elements of the fault feature vectors.

Table 2. Example feature vectors of the motor's rolling bearings under different operating conditions.

Scale factor	Normal condition	Inner ring fault	Rolling element fault	Outer ring fault
1	1.6811	0.8623	0.9468	0.7518
2	1.9158	0.9256	1.2205	1.0597
3	2.1957	1.1649	1.3644	1.0681
4	2.1351	1.3484	1.6182	1.5415
5	1.9212	1.1249	1.7236	1.3148
6	2.3512	1.2983	1.5311	1.0182
7	2.6235	1.4981	1.5184	1.7523
8	2.4266	1.7288	1.8256	1.8924
9	2.4512	1.6438	1.8467	1.8611
10	2.6381	1.6185	2.1066	1.5873
11	2.4463	1.6509	2.1849	1.4406
12	2.7239	1.7518	2.2206	1.5639
13	2.5846	1.6234	2.2691	1.7591
14	2.7391	1.7783	2.0312	1.8264
15	2.5368	1.7561	2.2283	1.9485
16	2.6631	1.7502	2.6429	1.6483
17	2.6619	1.6933	2.2718	1.7916
18	2.8893	1.7618	2.5364	1.9364
19	3.0198	1.8934	2.7618	1.9461
20	3.2264	1.8165	2.3648	2.0779

5.3 Identification results

Employing the fault feature extraction method based on EMD and MFE, 180 samples of fault feature vectors were obtained in this research. 100 of them were randomly selected as the training samples, while the remaining 80 were used as the testing set [32, 33]. The testing results are presented in **Table 3**.

Table 3. Classification results for motor rolling bearing fault diagnosis using different methods.

Feature extraction methods	Inner ring (%)	Rolling element (%)	Outer ring (%)	Normal condition (%)	Overall accuracy (%)
SVM	91.7	93.3	91.7	91.7	92.1
KELM	93.3	95	95	93	94.1
GWO-KELM	96.7	96.7	95	95	95.9
GWO-MKELM	98.3	100	100	100	99.6

As shown in **Table 3**, the GWO-MKELM method achieves the highest accuracy across all damage states. A comparison of overall accuracy reveals that the proposed method outperforms the SVM method by 7%, the KELM method by approximately 5%, and the GWO-KELM method by about 3%.

6. Conclusions

This study introduces a novel method for diagnosing motor rolling bearing faults by combining polynomial, perceptron, and Gaussian kernel functions with the GWO optimization algorithm to form the GWO-MKELM model. Experimental results showed that the new diagnostic method achieved a recognition accuracy of 99.3% across all fault states. This method outperformed traditional approaches, improving accuracy by nearly 7% over SVM, 5% over KELM, and 3% over GWO-KELM, proving its effectiveness in motor rolling bearing fault diagnosis.

References

[1] Wang, Y., Xue, C., Jia, X., et al., 2015. Fault diagnosis of reciprocating compressor valve with the method integrating acoustic emission signal and simulated valve motion. Mechanical Systems Signal Processing. 56–57, 197–212.

[2] Feng, G., Hu, N., Mones, Z., et al., 2016. An investigation of the orthogonal outputs from an on-rotor MEMS accelerometer for reciprocating compressor condition monitoring. Mechanical Systems Signal Processing. 76–77, 228–241.

[3] Chen, P., Zhao, X., Zhu, Q., 2020. A novel classification method based on ICGOA-KELM for fault diagnosis of rolling bearing. Applied Intelligence. 50, 2833–2847.

[4] Benmahamed, Y., Teguar, M., Boubakeur, 2017. Application of SVM and KNN to Duval Pentagonl for transformer oil diagnosis. IEEE Transactions on Dielectrics Electrical Insulation. 24(6), 3443–3451.

[5] Xiong, S., Zhang, H., Wang, M., et al., 2022. Distributed Data Parallel Acceleration-Based Generative Adversarial Network for Fingerprint Generation. Innovations in Applied Engineering and Technology. 1–12.

[6] Xiong, S., Zhang, H., Wang, M., 2022. Ensemble Model of Attention Mechanism-Based DCGAN and Autoencoder for Noised OCR Classification. Journal of Electronic & Information Systems. 4(1), 33–41.

[7] Lei, J., 2022. Green Supply Chain Management Optimization Based on Chemical Industrial Clusters. Innovations in Applied Engineering and Technology. 1–17.

[8] Lei, J., 2022. Efficient Strategies on Supply Chain Network Optimization for Industrial Carbon Emission Reduction. Journal of Computational Methods in Engineering Applications. 1–11.

[9] Wang, C., Ma, H., He, Y., et al., 2011. Adaptive approximate data collection for wireless sensor networks. IEEE Transactions on Parallel and Distributed Systems. 23(6), 1004–1016.

[10] Jiang, T., Li, Y., Li, S., 2023. Multi-fault diagnosis of rolling bearing using two-dimensional feature vector of WP-VMD and PSO-KELM algorithm. Soft Computing. 27(12), 8175–8187.

[11] Feng, Z., Deqiang, C., Xiong, S., et al., 2019. Method and apparatus for file identification. Google Patents.

[12] Fang, X.-L., Gao, H., Xiong, S.-G., 2012. RPR: High-reliable low-cost geographical routing protocol in wireless sensor networks. Journal of China Institute of Communications. 33(5).

[13] Cheng, C., Tay, W.P., Huang, G.-B., 2012. Extreme learning machines for intrusion detection. The 2012 International Joint Conference on Neural Networks (IJCNN).

[14] Huang, G.-B., 2014. An insight into extreme learning machines: random neurons, random features and kernels. Cognitive Computation. 6, 376–390.

[15] Yu, L., Li, J., Cheng, S., et al., 2013. Secure continuous aggregation in wireless sensor networks. IEEE Trans-

actions on Parallel and Distributed Systems. 25(3), 762–774.

[16] Wong, P.K., Yang, Z., Vong, C.M., et al., 2014. Real-time fault diagnosis for gas turbine generator systems using extreme learning machine. Neurocomputing. 128, 249–257.

[17] Lei, J., Nisar, A., 2023. Investigating the Influence of Green Technology Innovations on Energy Consumption and Corporate Value: Empirical Evidence from Chemical Industries of China. Innovations in Applied Engineering and Technology. 1–16.

[18] Xiong, S., Yu, L., Shen, H., et al., 2012. Efficient algorithms for sensor deployment and routing in sensor networks for network-structured environment monitoring. 2012 Proceedings IEEE INFOCOM. IEEE. 1008–1016.

[19] Chen, X., Zhang, H., 2023. Performance Enhancement of AlGaN-based Deep Ultraviolet Light-emitting Diodes with AlxGa1-xN Linear Descending Layers. Innovations in Applied Engineering and Technology. 1–10.

[20] Feng, Z., Xiong, S., Cao, D., et al., 2015. Hrs: A hybrid framework for malware detection. Proceedings of the 2015 ACM International Workshop on Security and Privacy Analytics. 19–26.

[21] Li, J., Yu, L., Gao, H., et al., 2011. Grouping-enhanced resilient probabilistic en-route filtering of injected false data in WSNs. IEEE Transactions on Parallel and Distributed Systems. 23(5), 881–889.

[22] Cheng, L., Li, S., 2015. Prediction of slope displacement based on PSO-KELM model with mixed kernel. Electronic Journal of Geotechnical Engineering. 20(3), 935–942.

[23] Yang, L., Jiang, Y., Liu, H., et al., 2022. Dimensional Error Prediction of Grinding Process Based on Bagging–GA–ELM with Robust Analysis. Machines. 11(1), 32.

[24] Sun, W., Wang, X., 2023. Improved chimpanzee algorithm based on CEEMDAN combination to optimize ELM short-term wind speed prediction. Environmental Science Pollution Research. 30(12), 35115–35126.

[25] Yu, L., Li, J., Cheng, S., et al., 2011. Secure continuous aggregation via sampling-based verification in wireless sensor networks. 2011 Proceedings IEEE INFOCOM. IEEE. 1763–1771.

[26] Xiong, S., Chen, X., Zhang, H., 2023. Deep Learning-Based Multifunctional End-to-End Model for Optical Character Classification and Denoising. Journal of Computational Methods in Engineering Applications. 1–13.

[27] Mirjalili, S., Mirjalili, S.M., Lewis, A., 2014. Grey wolf optimizer. Advances in Engineering Software. 69, 46–61.

[28] Haiyang, Z., Jindong, W., Lee, J., et al., 2018. A compound interpolation envelope local mean decomposition and its application for fault diagnosis of reciprocating compressors. Mechanical Systems Signal Processing. 110, 273–295.

[29] Alfadli, K.M., Almagrabi, A.O., 2023. Feature-Limited Prediction on the UCI Heart Disease Dataset. Computers, Materials Continua. 74(3), 5871–5883.

[30] Zhao, X., Qin, Y., He, C., et al., 2022. Underdetermined blind source extraction of early vehicle bearing faults based on EMD and kernelized correlation maximization. Journal of Intelligent Manufacturing. 33, 185–201.

[31] Cheng, H., Minghui, Z., 2021. Groundwater quality evaluation model based on multi-scale fuzzy comprehensive evaluation and big data analysis method. Journal of Water Climate Change. 12(7), 2908–2919.

[32] Shan, J.-n., Wang, H.-z., Pei, G., et al., 2022. Research on short-term power prediction of wind power generation based on WT-CABC-KELM. Energy Reports. 8, 800–809.

[33] Li, X., Zhao, H., 2022. Performance prediction of rolling bearing using EEMD and WCDPSO-KELM methods. Applied Sciences. 12(9), 4676–4683.